

¹⁹F Magnetic Resonance Imaging Enabled Real-time, Non-invasive and Precise Localization and Quantification of Degradation Rate of Hydrogel Scaffolds *In Vivo*

Qinghua Li,^{a,bl} Zujian Feng,^{a,bl} Huijuan Song,^b Jianhua Zhang,^{a*} Anjie Dong,^a Deling Kong,^{bc} Weiwei Wang,^{b*} Pingsheng Huang^{b*}

^a Department of Polymer Science and Technology, School of Chemical Engineering and Technology, Tianjin University, Tianjin 300072, China

^b Tianjin Key Laboratory of Biomaterial Research, Institute of Biomedical Engineering, Chinese Academy of Medical Sciences and Peking Union Medical College, Tianjin 300192, China

^c The Key Laboratory of Bioactive Materials, Ministry of Education; College of Life Science, Nankai University, Tianjin 300071, China

*Corresponding Author

E-mail: jhuazhang@tju.edu.cn; wwwangtj@163.com; sheng1989.2008@163.com.

Content

1. Materials and experimental methods	1
1.1 Materials	1
1.2 Synthesis and characterization of PA-CBF ₃ molecule.....	1
1.3 Synthesis and characterization of the PA-CBF ₃ labeled hydrogel materials	4
1.3.1 The synthesis method.....	4
1.3.2 The influence of ¹⁹ F labeling on the gelation behavior of PEV hydrogel	5
1.4 The ¹⁹ F NMR properties of CBF ₃ -PEV hydrogel materials	6
1.4.1 The calculation of fluorine content in the CBF ₃ -PEV hydrogel materials	6
1.4.2 Evaluation of ¹⁹ F NMR properties of CBF ₃ -PEV polymer	6
1.4.3 ¹⁹ F MRI of CBF ₃ -PEV hydrogel <i>in vitro</i>	7
1.5 The biocompatibility of ¹⁹ F labelling.....	8
1.5.1 Cytotoxicity analysis.....	8
1.5.2 Hematological analysis	8
1.5.3 Histological evaluation	9
1.6 The ¹⁹ F MRI <i>in vivo</i> after subcutaneous injection of volume-gradient dose	9
1.7 The fluorescence labelling with Cy7 and <i>in vivo</i> imaging after subcutaneous injection of volume-gradient dose.....	11
1.8 The establishment of quantitative algorithm and tracking the real-time degradation behavior.....	12
1.9 The facile applicability of ¹⁹ F labelling for multiple types of materials.....	13
1.10 Ethics of animal experiments.....	14
2. Experimental results	15
Figure s1. The MRS of intermediates and PA-CBF ₃ final product.	15
Figure s2. The mass spectrum of PA-CBF ₃ molecule.	16
Figure s3. The ¹⁹ F MRS of CBF ₃ -PEV polymer as a function of concentration or in biological samples.....	17
Figure s4. The evaluation of biocompatibility based on cytotoxicity and blood routine examination	18
Figure s5. Histological analysis of major organs and skin tissues.....	19
Figure s6. The fluorescence emission spectra of Cy7 and Cy7-labelled PEV polymer.	20
References	20

1. Materials and experimental methods

1.1 Materials

2-propynylamine (PA), 2, 4-dinitrobenzenesulfonyl chloride (DNBS), 3, 3, 3-trifluoro-1-propanol, triphenylphosphine (Ph₃P), diethyl azodicarboxylate (DEAD), 2-thioglycolic acid, formic acid, formaldehyde, *tert*-butyl bromoacetate, trifluoroacetic acid (TFA), triethylsilane, 2, 2-azobisisobutyronitrile(AIBN) were purchased from J&K chemical company. Alginate, poloxamer, 3-chloropropylamine hydrochloride, sodium azide (NaN₃), methanesulfonyl chloride (MsCl), acrylylchloride, acrylamide, sodium ascorbate and anhydrous cupric sulfate were purchased from Sigma-Aldrich. Anhydrous Trimethylamine (TEA), dichloromethane (DCM), tetrahydrofuran (THF) and *N, N*-dimethylformamide (DMF) were purchased from Sigma-Aldrich. α -Amino-*o*-methoxy poly(ethylene glycol) (mPEG-NH₂, *Mn* = 2000 g/mol) and azide-NH₂ (*Mn* = 2000 g/mol) were purchased from JenKem Technology Co.,Ltd. L-Valine *N*-carboxy anhydrides (L-val NCAs) were custom-made by Chengdu Enlai biological technology Co.,Ltd. Sulfo-Cyanine7 NHS ester was purchased from Xian Ruxi Biological Technology Co., Ltd.

1.2 Synthesis and characterization of PA-CBF₃ molecule

The PA-CBF₃ molecule was synthesized by multi-step method. Firstly, PA-DNBS (1) were prepared from 2, 4-dinitrobenzenesulfonyl chloride (DNBS) and 2-propynylamine, using TEA as the acid scavenger. PA (2.75 g, 38.6 mmol) was dispersed in anhydrous THF (50 mL), which was added with TEA (11.74 g, 116 mmol) at 0 °C. After stirring for 15 min, DNBS (12.39 g, 46.4 mmol) dissolved in anhydrous THF was added dropwise to the reaction mixture. After reacted for another

Supporting Information

24 h, the reaction mixture was filtered to obtain the filtrate, during which the triethylamine hydrochloride (solid) was removed. The organic solvents were removed by rotary evaporation. Then, the crude product was purified by silica gel chromatography with 20% hexane in dichloromethane, and afforded the product as light yellow solid (9 g, 60% yield). ¹H NMR (400 MHz, CDCl₃-d) δ 8.72 (t, J = 9.5 Hz, 1H), 8.62 - 8.50 (m, 1H), 8.44 (d, J = 8.6 Hz, 1H), 4.09 (dd, J = 6.4, 2.5 Hz, 2H), 2.01 (t, J = 2.5 Hz, 1H).

Secondly, 2, 4-dinitro-N-(prop-2-yn-1-yl) benzenesulfonamide (PA-DNBS-CF₃) (2) was synthesized using Mitsunobu reaction. In detail, to the solution of (1) (2.91g, 10.2 mmol) in anhydrous THF (50 mL) was added Ph₃P (5.34g, 20.4 mmol) and 3, 3, 3-trifluoro-1-propanol (2.327 g, 20.4 mmol) at 0 °C. After stirring for 15min, 10 mL of DEAD (3.55 g, 20.4 mmol) solution were added dropwise to the reaction mixture. After reacted for another 24 h at 25 °C, the reaction mixture was added hexane dropwise until turbidity point, which was stored at -20 °C for another 12 h. The precipitated triphenylphosphine oxide by-product was removed by filtration. The organic solvents were removed by rotary evaporation. Then, the crude product was purified by silica gel chromatography with 20% hexane in ethyl acetate. Product was obtained as a light yellow solid (3.6g, 70% yield). ¹H NMR (400 MHz, CDCl₃-d) δ 8.47 (ddd, J = 89.0, 47.8, 5.4 Hz, 3H), 4.26 (d, J = 2.4 Hz, 2H), 3.70 (dd, J = 8.4, 6.6 Hz, 2H), 2.65 - 2.44 (m, 2H), 2.30 (t, J = 2.5 Hz, 1H).

Thirdly, N-(3, 3, 3-trifluoropropyl)prop-2-yn-1-amine (PA-CF₃-NH) (3) were prepared from 2-thioglycolic acid, using TEA as the acid scavenger. (2) (2.5 g, 6.6 mmol) was dispersed in anhydrous DCM (50 mL), which was added with TEA (1.33 g, 13.2 mmol) at 0 °C. After stirring for 15 min, the 2-thioglycolic acid (783 mg, 8.5 mmol) was added dropwise to the reaction mixture. After reacted for another 30 min,

Supporting Information

the reaction mixture was precipitated in ice-cold ether. Then, the mixture was stored at -20 °C for another 12 h. The reaction mixture was filtered to obtain the filtrate. The organic solvents were removed by rotary evaporation. Then, the crude product was purified by silica gel chromatography with 20% hexane in dichloromethane, and afforded the product as light yellow oil (2g, 80% yield). ¹H NMR (400 MHz, CDCl₃-*d*) δ 3.45 (d, J = 2.4 Hz, 2H), 2.96 (t, J = 7.2 Hz, 2H), 2.39 - 2.27 (m, 2H), 2.25 (dd, J = 4.9, 2.5 Hz, 1H).

Subsequently, N-methyl-N-(3,3,3-trifluoropropyl)prop-2-yn-1-amine (PA-CF₃-N) (4) was synthesized by refluxing in formic acid and formaldehyde in oil bath at 70 °C under nitrogen protection for 48 h. The reaction mixture was adjusted to weakly basic with NaOH, and then the solution was extracted with ethyl acetate. The organic solvents were collected and removed by rotary evaporation. Then, the crude product was used without further purification due to the low boiling point (1.8 g, 90% yield).

Then, N-(2-(tert-butoxy)-2-oxoethyl)-N-methyl-N-(3, 3, 3-trifluoropropyl) prop-2-yn-1-aminium (PA-CB(*tbu*)F₃) (5) was synthesized by reacting (4) (1 g, 6.1 mmol) with tert-Butyl bromoacetate(1.42 g, 7.3 mmol) in acetonitrile at 50 °C. The organic solvents were removed by rotary evaporation. Then, the crude product was purified by silica gel chromatography with 5% dichloromethane in methanol, and afforded the product as white solid (1.2 g, 70% yield). ¹H NMR (400 MHz, CD₃OD) δ 4.64 (m, 2H), 4.44 (s, 2H), 4.08 - 3.92 (m, 2H), 3.70 (t, J = 2.5 Hz, 1H), 3.40 (s, 3H), 3.04 - 2.89 (m, 2H), 1.55 (s, 9H).

Finally, the deprotection of *tert*-butyl was conducted. The PA-CB(*tbu*)F₃ (5) (5 mmol) was dissolved in a mixed solution of anhydrous DCM and TFA (V_{DCM} : V_{TFA} =1:1), to which triethylsilane (12.5 mmol) was added. The reaction was allowed to continue for 2 h at RT, following which DCM and TFA were removed under vacuum.

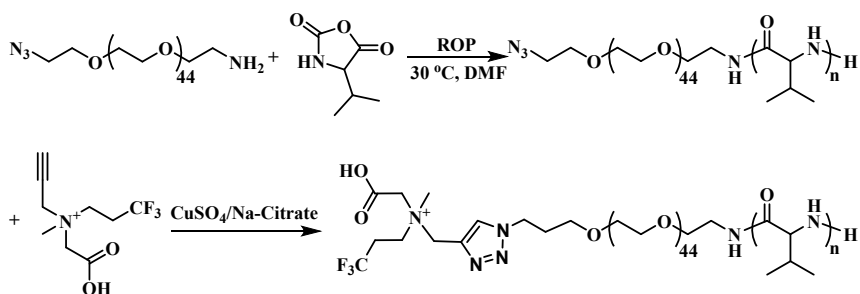
Supporting Information

The viscous crude product was washed with diethyl ether. The precipitate was collected and dried under vacuo to obtain white solid product (PA-CBF₃, 87% yield). ¹H NMR (400 MHz, D₂O) δ 4.51 (d, *J* = 2.4 Hz, 2H), 4.16 (s, 2H), 4.02 - 3.84 (m, 2H), 3.28 (s, 3H), 3.22 (t, *J* = 2.4 Hz, 1H), 2.83 (dd, *J* = 17.4, 9.6 Hz, 2H). ¹³C NMR (100 MHz, D₂O) δ 167.01, 125.06 (q, *J* = 274.5 Hz), 82.61, 70.13, 59.98, 55.63, 53.46, 49.26, 27.34 (q, *J* = 274.5 Hz). LCMS, calc'd *m/z* for C₉H₁₃F₃NO₂: 224.0898, found: 224.0902.

1.3 Synthesis and characterization of the PA-CBF₃ labeled hydrogel materials

1.3.1 The synthesis method

According to our previously reported protocol, N₃-PEG-*b*-poly(L-valine) (N₃-PEV) and mPEG-*b*-poly(L-valine) (PEV) copolymers were prepared by the ring opening polymerization (ROP) of L-Val NCAs in the presence of N₃-PEG-NH₂ or mPEG-NH₂, respectively.^{1, 2} Briefly, N₃-PEG-NH₂ (1.0 g, 0.5 mmol) was dissolved in anhydrous DMF (15 mL) under the protection of argon. Then, L-Val NCAs (357.5 mg, 2.5 mmol) were added to the flask, and the reaction was continued at 30 °C for 72 h. The resulting mixture was dialyzed against distilled water for 48 h using a dialysis bag (molecular weight cut off, 1000 Da). After freeze-drying, white powder of N₃-PEV copolymer was obtained. Subsequently, CBF₃-PEV copolymer was synthesized by conjugating PA-CBF₃ molecule to the N₃-PEV copolymer through “click” reaction at 37°C for 24 h, using sodium ascorbate and anhydrous cupric sulfate as the catalyst.³⁻⁵ The copper ions were removed by dialyzing against distilled water for 48 h. After freeze-drying, white powder of CBF₃-PEV copolymer was obtained.



Scheme s1. The synthetic route of CBF₃-PEV copolymer.

1.3.2 The influence of ¹⁹F labeling on the gelation behavior of PEV hydrogel

The chemical composition of CBF₃-PEV copolymer was evaluated by ¹H NMR (Varian Unity, 500 MHz) using TFA-*d* as the solvent. The polydispersity index (PDI) of molecular weight of the copolymers was determined on a Waters Chromatography system equipped with a refractive index detector. A mobile phase of dimethylformamide containing 0.1% w/v LiBr was used with a flow rate of 1 mL/min at 70 °C. Poly(ethylene glycol) with a molecular weight ranging from 300 to 30000 Da was used as standards. FT-IR spectra of polymers were studied on an IR Prestige 21 system (Shimadzu Corporation, Japan) and analyzed using IR solution v.1.40 software. The ellipticity of CBF₃-PEV and PEV copolymer aqueous solutions (0.1 mg/mL) was measured using a circular dichroism instrument (J-810, JASCO) at 37 °C. The ultraviolet region was scanned between 190 and 400 nm for three times. In addition, rheological analysis was investigated using AR 2000ex rheometer (TA) with a circulating environment system for temperature control. The CBF₃-PEV and PEV polymer aqueous solution in the gel state at a concentration of 100 mg/mL was placed between parallel plates with a diameter of 25 mm and a gap of 0.5 mm. The measurements of elasticity modulus (*G'*) and viscosity modulus (*G''*) were carried out over a frequency sweep between 0.1 and 100 rad/s, a time sweep of 30 min, and a strain sweep from 0.1 to 10.0 at 37 °C. Scanning electron microscopy (SEM) was used

to observe morphological characteristics. The CBF₃-PEV hydrogel was quenched in liquid nitrogen and freeze-dried. SEM images were obtained using a field emission scanning electron microscopy instrument (Hitachi S-4800).

1.4 The ¹⁹F NMR properties of CBF₃-PEV hydrogel materials

1.4.1 The calculation of fluorine content in the CBF₃-PEV hydrogel materials

The calculation of fluorine content in the CBF₃-PEV hydrogel materials was performed using the Bruker's 'Digital ERETIC' tool package.⁶⁻⁸ In detail, CBF₃-PEV polymer was dissolved in PBS at a concentration of 5 mg/mL, of which the ¹⁹F MRS were detected by Bruker Avance 400 (TopSpin™ 3.5) instrument. The number of scans was maintained at 64. Subsequently, the concentration measurements of PA-CBF₃ labeled hydrogel materials To calculate the concentration of a given sample (termed as X) referenced to the Digital ERETIC signal, we used the following equation:

$$^{19}\text{F content in the hydrogel materials} = \frac{I_{\text{F}} \times C_{\text{ERETIC}}}{C_{\text{polymer}} \times I_{\text{ERETIC}}} \times 100\% \quad (1)$$

In *equation (1)*: I_{polymer} , the signal intensity of the ¹⁹F MRS of ¹⁹F labeled hydrogel materials; C_{polymer} : the concentration of the ¹⁹F labeled hydrogel materials (mg/mL); I_{ERETIC} , the signal intensity of the ¹⁹F MRS of the Digital ERETIC; C_{ERETIC} , the concentration of ¹⁹F in Digital ERETIC sample (mg/mL); In this study, PA-CBF₃ was used as the Digital ERETIC.

1.4.2 Evaluation of ¹⁹F NMR properties of CBF₃-PEV polymer

The relaxation times was measured according to the *Handbook of nuclear magnetic*

Supporting Information

resonance, during which the sample temperature was maintained at 37 °C. The ^{19}F spin-lattice relaxation time (T_1) was measured using the standard inversion-recovery pulse sequence. The ^{19}F spin-spin relaxation time (T_2) was determined using the Carr-Purcell-Meiboom-Gill (CPMG) pulse sequence. Samples in PBS (10 mM, pH = 7.4) containing 10 % D_2O was used as the control. The vclist and vdlist were set according to a exponential change. T_1 value could be read directly in the fitting report. T_2 value is calculated by the following equation: $T_2 = \text{Fitting cycle number} \cdot (2D_{20} + P_2)$. Then, the relaxation time of $\text{CBF}_3\text{-PEV}$ polymer as a function of concentration was measured using the above stated protocol. The samples of concentration gradient (1 - 100 mg/mL) were prepared in DI water containing 10 % D_2O .

Subsequently, the $\text{CBF}_3\text{-PEV}$ polymer (10 mg/mL) were incubated with blood plasma and tissue homogenate (heart, liver, spleen, lung and kidney) at 37 °C for 48 h. The ^{19}F MRS peaks was acquired on on Bruker Avance 400 MHz (TopSpin™ 3.5). The number of scans was maintained at 64. The chemical shift, signal-to-noise ratio (SNR), and full width at half maximum (FWHM) were measured. The number of scans was maintained at 64. The signal to noise ratio were calculated by the “.sino” command. The relaxation time was measured using the above stated protocol.

1.4.3 ^{19}F MRI of $\text{CBF}_3\text{-PEV}$ hydrogel *in vitro*

The ^{19}F MRI images were obtained on the 7.0T 200 mm transverse-bore microimaging system (Bruker BioSpec 70/20 USR). ^{19}F MR images were acquired using a 2D *TI* RARE sequence with $\text{TR/TE} = 3000/4.6$ ms, $\text{FA} = 90$, $\text{FOV} = 50 \times 50$ mm, $\text{MTX} = 90 \times 90$, slice thickness = 4 mm, number of averages = 40. In the process of signal acquisition, the sample temperature was controlled by circulating

thermostatic water bath, which was maintained at 37 °C. The ^{19}F MRI images were processed using the MRIcroGL software, where the color bar represented the signal intensity.

$$SI = M19F \left(1 - 2 \times e^{\left(-\frac{TI}{T1}\right)} + e^{\left(-\frac{TR}{T1}\right)} \right) \times e^{\left(-\frac{TE}{T2}\right)} \quad (2)$$

In equation (2): SI , signal intensity; $M19F$, magnetization vector of ^{19}F ; TI , inversion time; TR , repetition time; TE , echo time.

1.5 The biocompatibility of ^{19}F labeling

1.5.1 Cytotoxicity analysis

The *in vitro* cytotoxicity analysis of PEV and $\text{CBF}_3\text{-PEV}$ polymer were evaluated on NIH 3T3 cells and dendritic cell 2.4 cell line. Culture media were supplemented with 10% heat-inactivated fetal bovine serum (FBS), penicillin (100 U/mL) and streptomycin (100 $\mu\text{g/mL}$). Cells were maintained in DMEM/High Glucose media (Hyclone) at 37 °C. Briefly, cells were seeded at a density of 5×10^4 cells/well in 96-well microtiter plates and pre-incubated for 24 h. Cells were then exposed to a series of 50 μL of polymer solutions with gradient concentrations. After incubation for 48 h, CCK-8 assay was carried out according to the standard protocol. The experiment was set up in quintuplicate to determine mean values and standard deviations (SDs).

1.5.2 Hematological analysis

Hematological examinations were performed by automatic blood analyzer (Celltace, Japan). The injection volume for each mouse was maintained at 200 μL ($n = 4$). The whole blood samples ($\sim 50 \mu\text{L}$) were collected into heparinized tube from orbital vein

at scheduled time points (1 week, 2 week, and 3 week post injection), which were subjected for hematological analysis.

1.5.3 Histological evaluation

In order to evaluate the toxicity of ^{19}F labeling in mice after subcutaneous injections, histological studies were also performed. Mice were sacrificed by cervical vertebra dislocation at scheduled time points (1 week, 2 week, and 3 week post injection). The major organs including heart, liver, spleen, lung, and kidney, and skin at the injection site were harvested immediately after the dissection. The tissues were immediately fixed with 10% formalin for 1 day at room temperature and embedded in paraffin. The embedded specimens were sectioned along the longitudinal axis of the tissues, and the sections were stained with hematoxylin and eosin (H&E) and observed using optical microscope. In addition, in order to observe the collagen deposition in the adjacent injection site, Masson's trichrome staining was conducted according to the standard protocol.

1.6 The ^{19}F MRI *in vivo* after subcutaneous injection of volume-gradient dose

For all *in vivo* imaging sessions, the body temperature and respiration rates of the animals were monitored using a rectal probe and a pressure sensitive pad placed underneath the thorax. A monitoring and gating model (type 1030) from SA Instruments (Stony Brook, NY, USA) was used to regulate and maintained the body temperature and respiration rate of the animal at reasonable physiological ranges of approximately $37\text{ }^{\circ}\text{C}$ and $80\text{-}120\text{ breaths min}^{-1}$, respectively.

Supporting Information

CBF₃-PEV hydrogel (100 mg/mL, 200 μL, 150 μL, 100 μL, 50 μL and 25 μL, respectively) were subcutaneously injected to the female BALB/c mice (non-shaving, n = 3), the ¹⁹F MRS/MRI experiments *in vivo* were conducted on the 7.0T 200 mm transverse-bore microimaging system (Bruker BioSpec 70/20 USR). First, whole-body ¹⁹F spectra were obtained after the “location” step. The spectra were acquired using FID pulse sequence with 100 averages, 1.6 s TR and 0.15 ms TE. Full wide bandwidth was used to monitor if there exists a second ¹⁹F MRS peak. Subsequently, the mice were imaged using a volume birdcage coil, which could be tuned to either 282 MHz for ¹⁹F or 300 MHz for ¹H. ¹⁹F MR images were acquired using a 2D *T1* RARE sequence with TR/TE = 3000/4.6 ms, FA = 90, FOV = 50*50 mm, MTX = 100*100, number of averages = 40, slice thickness = 4 mm. ¹H MR images were acquired using a 2D *T2* RARE sequence with TR/TE=300/50 ms, FA = 90, FOV = 50*50 mm, MTX = 256*256. The SNR ratios could be calculated from phantom images were estimated as average signal intensity in region of interest/standard deviation of signal intensity of background. The data were manipulated by interpolation (7th degree B-spline) using the Matlab 2010b software. Subsequently, the 3D rendering images and 2D coronal images were processed using the MRICroGL and MRICron software, respectively.

Then, the quantitative algorithms were established to calculate the total pixel volume (*TPV*) and total fluorine content (*TFC*). The calculation was performed on a per-slice basis. The noise magnitude, *N*, of the ¹⁹F MR image was determined by calculating the standard deviation of voxel values near the periphery of the image. Next, the

Supporting Information

magnitude signal value, SI , was calculated in region of interest (ROI) containing the ^{19}F . The voxels with $SI > 3.0N$ were calculated, which could be identified as containing actual ^{19}F MRI signal. The algorithm (according to the following equation) was implemented in MATLAB (MATLAB R2013a, MathWorks, Eindhoven, The Netherlands).

$$\text{Total pixel volume (TPV)} = \sum_{i=1}^n V_i \quad (3)$$

$$\text{Total fluorine content (TFC)} = \sum_{i=1}^n C_i \times V_i \quad (4)$$

In *equation (3&4)*: C_i , the concentration of CBF_3 in voxel- i ; V_i , the volume of voxel- i ; t , The number of voxels above the concentration threshold.

1.7 The fluorescence labeling with Cy7 and *in vivo* imaging after subcutaneous injection of volume-gradient dose

In order to make comparison between the current fluorescence imaging modality and ^{19}F MRI, the labeling with near-infrared fluorescence probe Cy7 was utilized as a positive control. The terminal primary amino group facilely reacted with sulfo-Cy7-NHS active ester in a high efficiency. The unreacted Cy7 was removed by dialyzing against DI water away from light for 48 h. The PEV-Cy7 polymer was obtained after lyophilization. The fluorescence spectra were measured on fluorescence spectrophotometer (Varian Cary Eclipse).

Subsequently, PEV-Cy7 hydrogel (100 mg/mL, 200 μL , 150 μL , 100 μL , 50 μL and 25 μL , respectively) were subcutaneously injected to the female BALB/c mice (non-shaving, $n = 3$; shaving, $n = 3$), of which the fluorescence signal were detected by the

Supporting Information

CRI Maestro imaging system (CRI Corporation, Woburn, MA, USA). Fluorescence imaging adopts NIR mode, during which the excitation wavelength is set at 745nm. *In vivo* spectral imaging ranging from 740 nm to 950 nm (in 10 nm steps) was carried out with an exposure time of 300 ms for each image frame. In addition, the shaved mice were also imaged from the reversed direction with the same setting of parameters. For quantitative comparison, background was removed by using the spectral unmixing software and the regions of interest (ROI) were drawn over site injected hydrogel. The total signal for each area was measured. Hydrogel was quantified using the CRI Maestro region of interest (ROI) analysis software that produced pixel signal values of total fluorescence signal (*TFS*) divided by exposure time (total signal/ms). Results were presented as means \pm SD. for a group of 3 animals.

1.8 The establishment of quantitative algorithm and tracking the real-time degradation behavior

The quantification of degradation behavior after subcutaneous injection was calculated directly from the *in vivo* MRI dataset. CBF₃-PEV hydrogel (100 mg/mL, 200 μ L) was subcutaneously injected to the female BALB/c mice (non-shaving, n = 3), the ¹⁹F MRS/MRI signals *in vivo* were acquired on the 7.0T 200 mm transverse-bore microimaging system (Bruker BioSpec 70/20 USR) at scheduled time point (1 week, 2 week, 3 week, 4 week), using the above stated parameters. The calculation was performed on a per-slice basis. The noise magnitude, *N*, of the ¹⁹F MR image was determined by calculating the standard deviation of voxel values near the periphery of

the image. Next, the magnitude signal value, SI , was calculated in region of interest (ROI) containing the ^{19}F . The voxels with $SI > 3.0N$ were calculated, which could be identified as containing actual ^{19}F MRI signal. Then, degradation rate was calculated according to the following equation, which was reflected by the variation of ^{19}F content in comparison with the initial injection amount. The algorithm (according to the following equation) was implemented in MATLAB (MATLAB R2013a, MathWorks, Eindhoven, The Netherlands).

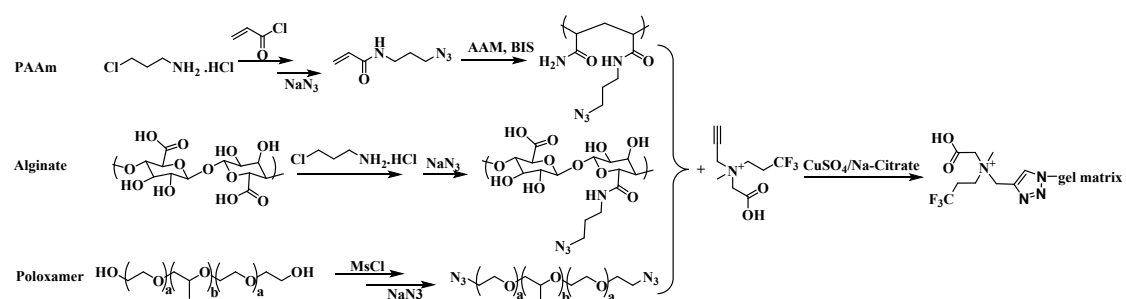
$$\text{Residual volume Ratio} = \frac{\sum_{i=1}^n C_i \times V_i}{V} \times 100\% \quad (5)$$

$$\text{Residual } ^{19}\text{F content Ratio} = \frac{\sum_{i=1}^n C_i \times V_i}{M} \times 100\% \quad (6)$$

In **equation (5&6)**: C_i ,

the concentration of CBF_3 in voxel- i ; V_i , the volume of voxel- i ; t , the number of voxels above the concentration threshold; V , the initial injection volume; M , the initial injection amount.

1.9 The facile applicability of ^{19}F labeling for multiple types of materials



Scheme s2. The synthetic route of ^{19}F labeled PAAM, alginate and poloxamer hydrogel matrix.

The ^{19}F labeling for multiple types of materials was typically conducted by major

Supporting Information

two steps, including azidation and “click” reaction. In terms of PAAm, *N*-(3-azidopropyl) acrylamide monomer was firstly synthesized using a two-step method, which was subsequently copolymerized with acrylamide to obtain the PAAm-N₃ polymer. As for alginate, the 3-chloropropylamine hydrochloride was conjugated *via* amidation reaction, which was further substituted with sodium azide through nucleophilic substitution reaction. The poloxamer was firstly modified with MsCl, which was then substituted with sodium azide. Finally, ¹⁹F labeled materials was synthesized by “click” reaction, using sodium ascorbate and anhydrous cupric sulfate as the catalyst. The copper ions were removed by dialyzing against distilled water for 48 h. After freeze-drying.

Subsequently, the ¹⁹F MRS, relaxation time and ¹⁹F MRI *in vitro* were implemented according the above stated protocols.

1.10 Ethics of animal experiments

All animals were purchased from Cancer Institute and Hospital, Chinese Academy of Medical Sciences. The animal experiment was performed in accordance with the protocol approved by the Chinese Academy of Medical Sciences and Peking Union Medical College.

2. Experimental results

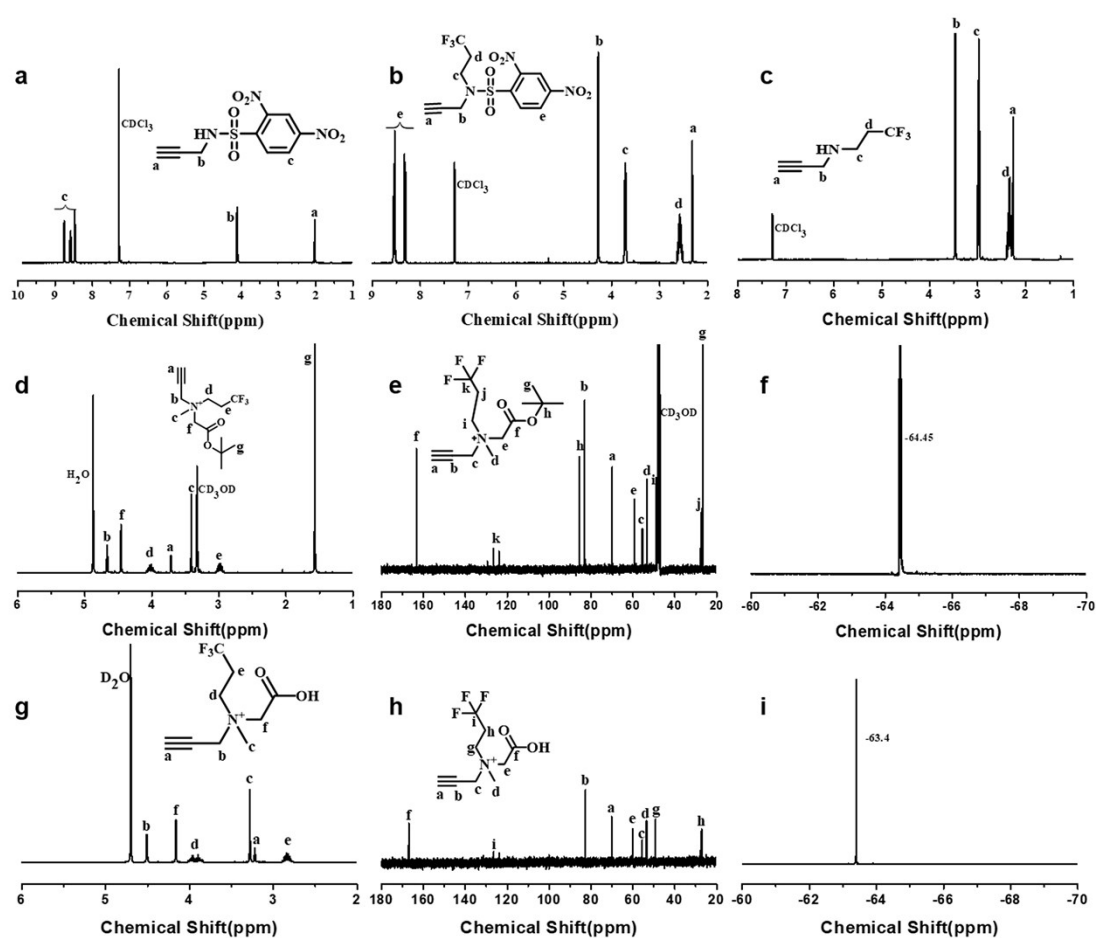
Figure s1. The MRS of intermediates and PA-CBF₃ final product.Figure s1. The MRS of intermediates and PA-CBF₃ final product.

Figure s2. The mass spectrum of PA-CBF₃ molecule.

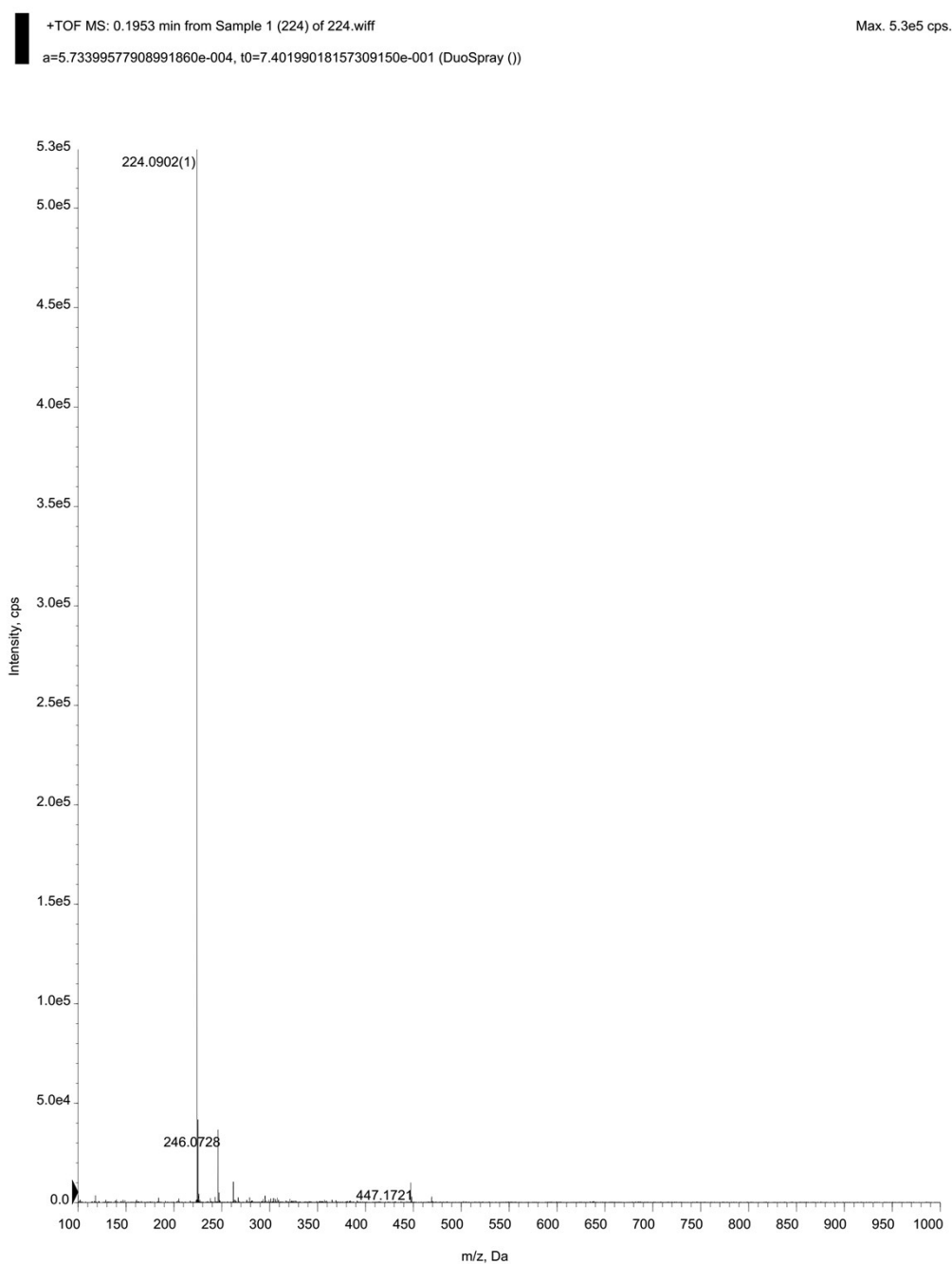


Figure s2. The mass spectrum of PA-CBF₃ molecule.

Figure s3. The ^{19}F MRS of $\text{CBF}_3\text{-PEV}$ polymer as a function of concentration or in biological samples.

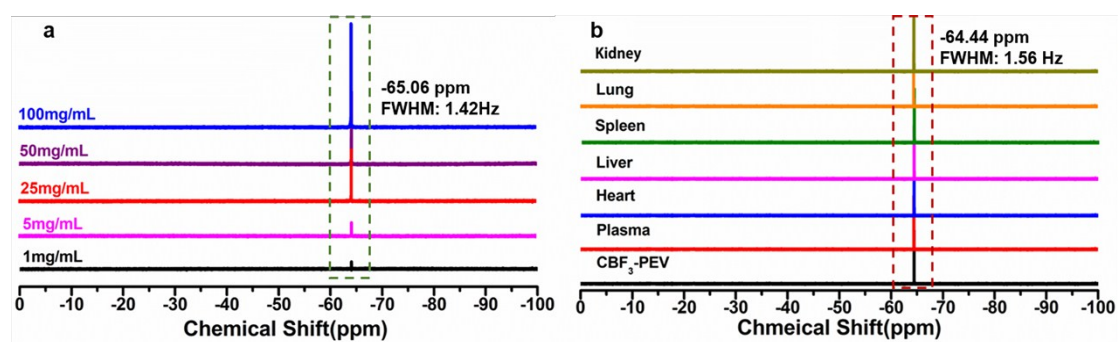


Figure s3. (a) ^{19}F MRS and FWHM of $\text{CBF}_3\text{-PEV}$ polymer as a function of concentration. (b) ^{19}F MRS and FWHM of $\text{CBF}_3\text{-PEV}$ polymer in plasma and tissue homogenate, including heart, liver, spleen, lung and kidney.

Figure s4. The evaluation of biocompatibility based on cytotoxicity and blood routine examination

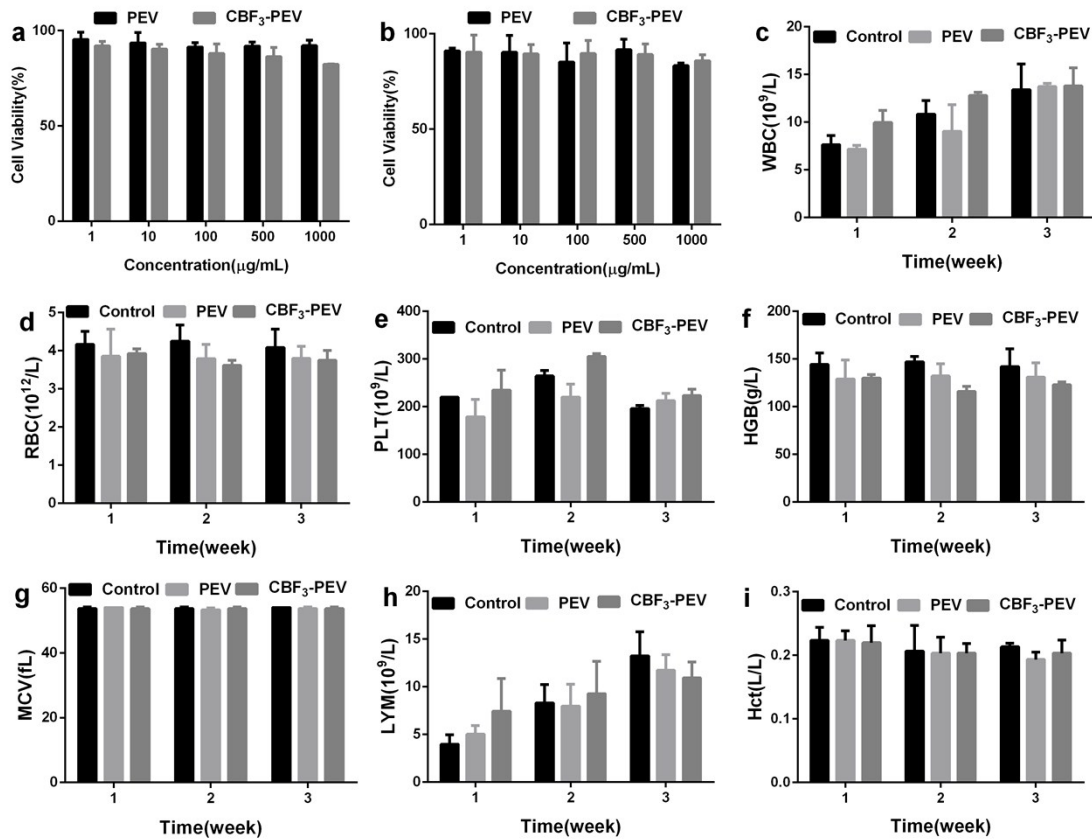


Figure s4. (a) The cytotoxicity of PEV and CBF₃-PEV polymer, evaluated on NIH 3T3 cells and (b) DC 2.4. Error bars represent the standard deviation, n = 4. (c) white blood cells (WBC), (d) red blood cells (RBC), (e) platelet (PLT), (f) hemoglobin (HGB), (g) mean corpuscular volume (MCV), (h) Lymphocyte ratio (LYM); hematocrit (Hct). The results were shown as mean ± standard deviation (n = 3).

Figure s5. Histological analysis of major organs and skin tissues.

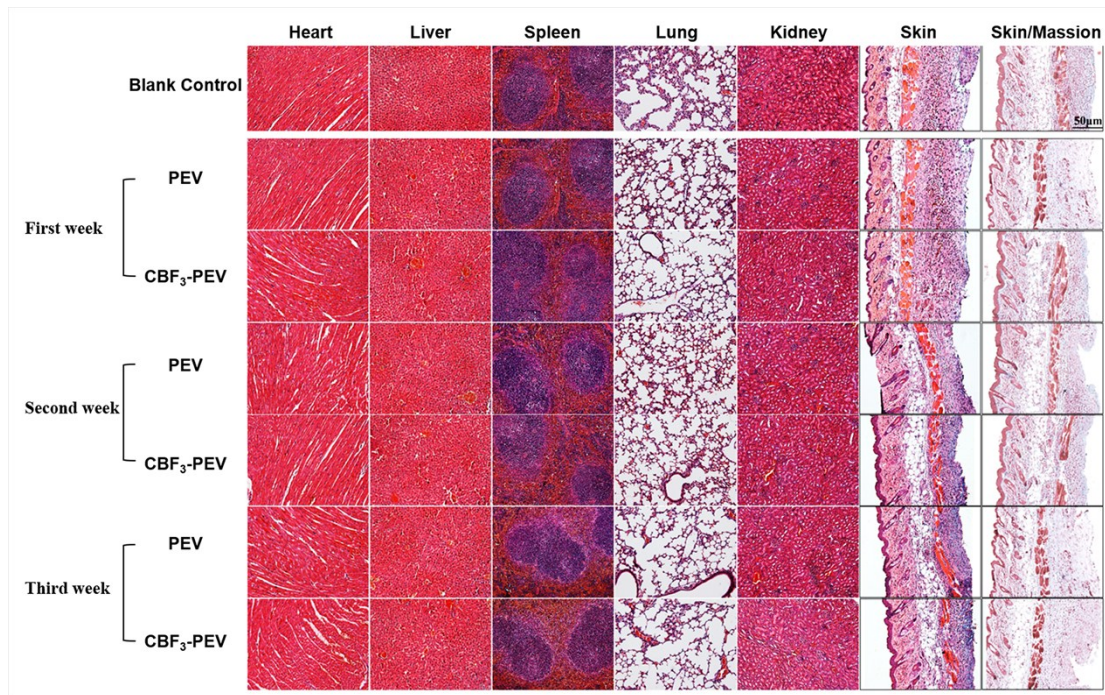


Figure s5. Histological analysis of major organs and skin tissues harvested from mice at scheduled timepoint (first week, second week and third week) after subcutaneous injection of PEV and CBF₃-PEV hydrogel, respectively. The scale bar is 50 µm.

Figure s6. The fluorescence emission spectra of Cy7 and Cy7-labelled PEV polymer.

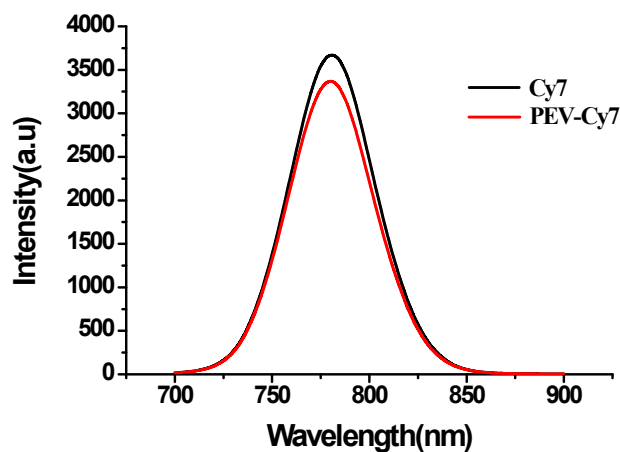


Figure s6. The fluorescence emission spectra of Cy7 and Cy7-labelled PEV polymer (termed as PEV-Cy7).

References

1. H. Song, P. Huang, J. Niu, G. Shi, C. Zhang, D. Kong and W. Wang, *Biomaterials*, 2018, **159**, 119-129.
2. H. Song, G. Yang, P. Huang, D. Kong and W. Wang, *J. Mater. Chem. B*, 2017, **5**, 1724-1733.
3. M. Arslan, G. Acik and M. A. Tasdelen, *Poly. Chem.* 2019, **10**, 3806-3821.
4. W. H. Binder and R. Sachsenhofer, *Macromol. Rapid Commun.* 2007, **28**, 15-54.
5. H. C. Kolb, M. G. Finn and K. B. Sharpless, *Angew. Chem., Int. Ed.* 2001, **40**, 2004-2021.
6. C. H. Cullen, G. J. Ray and C. M. Szabo, *Magn. Reson. Chem.* 2013, **51**, 705-713.
7. D. A. MacIntyre, B. Jiménez, E. J. Lewintre, C. R. Martín, H. Schäfer, C. G. Ballesteros, J. R. Mayans, M. Spraul, J. García-Conde and A. Pineda-Lucena, *Leukemia*, 2010, **24**, 788.
8. M. J. Albers, T. N. Butler, I. Rahwa, N. Bao, K. R. Keshari, M. G. Swanson and J. Kurhanewicz, *Magn. Reson. Med.* 2009, **61**, 525-532.